



Higher Order Temperature Dependence of SiPM used in FACT

Conference Paper

Author(s):

Hildebrand, Dorothée; [Ahnen, Max Ludwig](#) ; Adam, Jan; Balbo, Matteo; Biland, Adrian; Baack, Dominik; Bretz, Thomas; Buss, Jens; Blank, Michael; Einecke, Sabrina; Brügge, Kai; Dorner, Daniela; Elsässer, Dominik; Hempfling, Christina; Herbst, Tina; Mahlke, Max; Mannheim, Karl; Neise, Dominik; Neronov, Andrii; Nöthe, Maximilian; Paravac, Aleksander; Paus, Felicitas; Rhode, Wolfgang; Sliusar, Vitalii; Temme, Fabian; Thaele, Julia; Kortmann, Lukas; Dmytriiev, Anton; Linhoff, Lena; [Müller, Sebastian](#) ; Oberkirch, Jonas; Schleicher, Bernd; Schulz, Florian; Shukla, Amit

Publication date:

2018

Permanent link:

<https://doi.org/10.3929/ethz-b-000318086>

Rights / license:

[Creative Commons Attribution-NonCommercial-NoDerivatives 4.0 International](#)

Originally published in:

PoS: Proceedings of Science 301, <https://doi.org/10.22323/1.301.0778>

Higher Order Temperature Dependence of SiPM used in FACT

D. Hildebrand^a, J. Adam^b, M. L. Ahnen^a, D. Baack^b, M. Balbo^c, A. Biland^{*a}, M. Blank^d, T. Bretz^{a,1}, K. Bruegge^b, J. Buss^b, A. Dmytriiev^c, D. Dorner^d, S. Einecke^b, D. Elsaesser^b, C. Hempfling^d, T. Herbst^d, L. Kortmann^b, L. Linhoff^b, M. Mahlke^{a,1}, K. Mannheim^d, S. A. Mueller^a, D. Neise^a, A. Neronov^c, M. Noethe^b, J. Oberkirch^b, A. Paravac^d, F. Pauss^a, W. Rhode^b, B. Schleicher^d, F. Schulz^b, A. Shukla^d, V. Sliusar^c, F. Temme^b, J. Thaele^b, R. Walter^c

E-mail: dorothee.hildebrand@phys.ethz.ch

^aETH Zurich, Institute for Particle Physics

Otto-Stern-Weg 5, 8093 Zurich, Switzerland

^bTU Dortmund, Experimental Physics 5

Otto-Hahn-Str. 4, 44221 Dortmund, Germany

^cUniversity of Geneva, ISDC Data Center for Astrophysics

Chemin d'Ecogia 16, 1290 Versoix, Switzerland

^dUniversität Würzburg, Institute for Theoretical Physics and Astrophysics

Emil-Fischer-Str. 31, 97074 Würzburg, Germany

¹also at RWTH Aachen University

Solid state photosensors, usually called SiPM or G-APD, seem ideal devices to be used in Imaging Atmospheric Cherenkov Telescopes (IACT). Nevertheless, their temperature dependence poses questions about their suitability in the harsh environment intrinsic to the operation of IACTs. While detailed measurements in the laboratory are possible with some sample sensors, limited data about the performance and uniformity of large samples exist. The First G-APD Cherenkov Telescope (FACT) is pioneering the usage of SiPMs for IACTs. Its camera consists of 1440 SiPMs and it is operated since October 2011 each night when observation conditions permit. Using no temperature stabilization system for the sensors, their temperature is closely coupled to the outside temperature that can change by more than 20 °C. While the strong temperature dependence of the gain of the sensors was shown to be easily compensated by adapting the applied voltage, there could also be higher order temperature dependencies of parameters like optical cross-talk, after-pulsing and wavelength dependent photon-detection efficiency. While external calibration devices could be used, one would have to prove that these devices do not have their own temperature dependencies. Instead, we use the constant flux of high energetic cosmic ray particles as calibration device. Their measured flux can depend on variable absorption and scattering of Cherenkov light e.g. due to dust and clouds, as well as on seasonal variations of the atmosphere. Nevertheless, using data sets where the temperature drastically changed within short time periods, we show that temperature dependencies of FACT, including the SiPMs, are well under control.

35th International Cosmic Ray Conference — ICRC2017

10–20 July, 2017

Bexco, Busan, Korea

*Speaker.

1. Introduction

Imaging Atmospheric Cherenkov Telescopes (IACT) measure the faint flashes emitted by showers of secondary particles produced when a high energetic charged cosmic ray particle or gamma-ray interacts with the atmosphere. Therefore, IACTs need large mirror areas and fast photo sensors with high sensitivity. Usually, PhotoMultiplier Tubes (PMT) are used as photo sensors. But since few years, solid state sensors with comparable performance are available. These Geiger-mode operated Avalanche Photo Diodes (G-APD, also known as SiPM) are considered as suitable sensors for future IACTs. To investigate their feasibility and long-term behavior under the harsh conditions intrinsic to the operation of IACTs, the First G-APD Cherenkov Telescope (FACT) was constructed[1]. It consists of a camera with 1440 pixels of $3 \times 3 \text{ mm}^2$ Hamamatsu MPPC S10362-33-50C G-APD chips installed on a refurbished mount of a HEGRA telescope with a mirror area of $\approx 9.5 \text{ m}^2$. Since October 2011, FACT is taking data whenever observation conditions permit.

One key feature of SiPM is that several of their performance parameters like gain, optical crosstalk and wavelength-dependent photo detection efficiency (PDE) depend strongly on the applied overvoltage. But the total voltage to be applied depends on the temperature of the sensor. One possibility would be to install a temperature stabilization system. But in FACT, a different approach was taken [2]: The sensors are glued to solid light guides that are glued to the entrance window. The sensor compartment is (to some extent) thermally decoupled from the electronics compartment of the camera by a baffle plate. The electronics compartment is water cooled, with a heat exchange to the ambient air¹. Therefore, the temperature of the sensors is highly correlated with the ambient temperature (see figure 1).

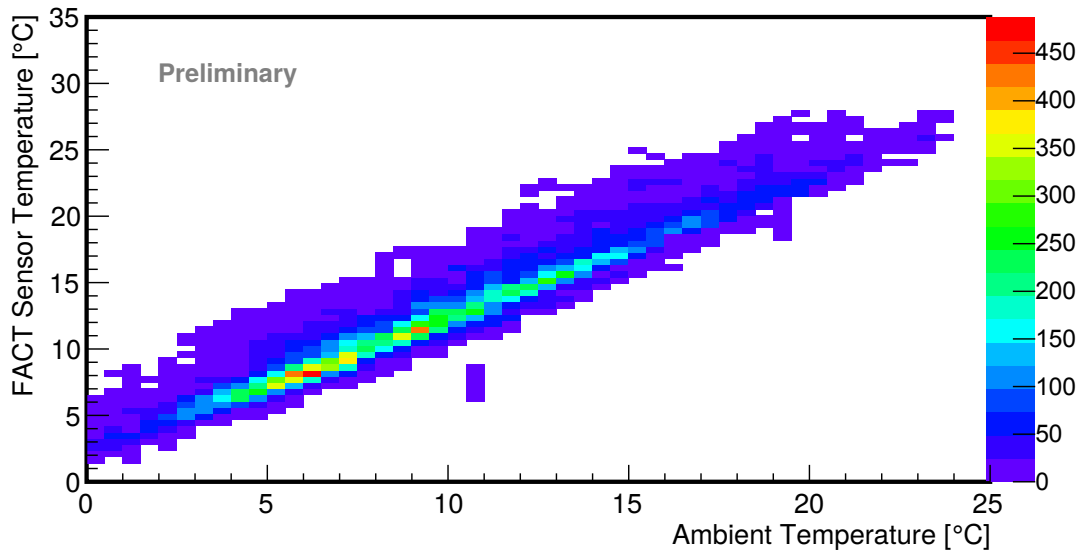


Figure 1: Correlation between ambient temperature and temperature of the SiPM sensors in the FACT camera. The sensors get warmer than usual if they are heated by the DC current due to strong ambient light.

¹In addition, a heating system is activated when necessary to prevent freezing.

It was measured during the commissioning of FACT at La Palma that the gain of the SiPM changes by $\approx 5\%$ per $^{\circ}\text{C}$ [2]. 28 temperature sensors² sample the temperature distribution on the sensor plate, and the voltage applied to each group of four or five neighboring pixels is adjusted every 15 seconds to ensure a constant gain over the full temperature range. Due to serial resistors between the power supply and the sensors, a voltage correction for the actual DC current also has to be taken into account. This correction is calculated and applied every three seconds, fast enough to cope with stars in the field of view during standard operation [2].

These corrections for temperature and DC current are sufficient to keep the performance of the FACT camera very stable and homogeneous without the need for any external calibration device.

Nevertheless, it is not a priori clear that there exist no other temperature effects. An expected temperature effect is the amount of dark noise signals from the sensors. But even at 30°C (the highest temperatures reached during operation so far) the dark noise rate is smaller than the signal rate due to ambient light that is measured to be about 30 million photo-electrons per second per FACT pixel during dark nights.

2. The Method

One could illuminate the SiPM sensors with different wavelengths at different temperatures in the laboratory and measure their performance. But this needs a dedicated setup and can usually only be performed for a small sample of sensors. Instead, we use standard data measured with FACT. For this, we apply the virtual trigger rate method described in [3]. It uses the stable and isotropic flux of high energetic charged cosmic ray particles that induce air-showers when interacting with the atmosphere. The trigger threshold of FACT during data taking is optimized to record also faint flashes. Therefore, some fraction of recorded events are due to statistical fluctuations of the ambient light. To ensure having a clean sample of events triggered by air-showers, the trigger logic is emulated in software and applied to recorded data. The FACT trigger consists of an analogue sum of the signal from nine adjacent pixels. So the software trigger is applied to the similar sum of the calibrated recorded signals from same adjacent pixels. It is now possible to set this software trigger to any value (larger than the hardware threshold during data taking) and calculate a virtual trigger rate. For FACT, applying a virtual trigger threshold of 700 mV, corresponding to about 70 photo-electrons in nine neighboring pixels within few ns, results in a rate that should not depend on the amount of ambient light and hardly depends on the zenith distance up to $\approx 40^{\circ}$ [3].

One cannot just compare the virtual trigger rate for different sensor temperatures, since there exists a systematic seasonal variation of the rate [3] that is visible in a shift of the virtual trigger rates seen in the following figures³.

Nevertheless, we identified two data periods where the sensor temperature changed drastically within about ten days, and there exists no indication for a significant systematic variation on this time scale. These data sets are in December 2015 and April 2016, respectively⁴.

²31 sensors are installed, but three of them are malfunctioning.

³The characterization of the seasonal variation is beyond the topic of this proceeding.

⁴Exact time periods are: 2015.12.09 - 2015.12.18 (MJD 57365 - 57377) and 2016.04.27 - 2016.05.07 (MJD 57505 - 57515), respectively.

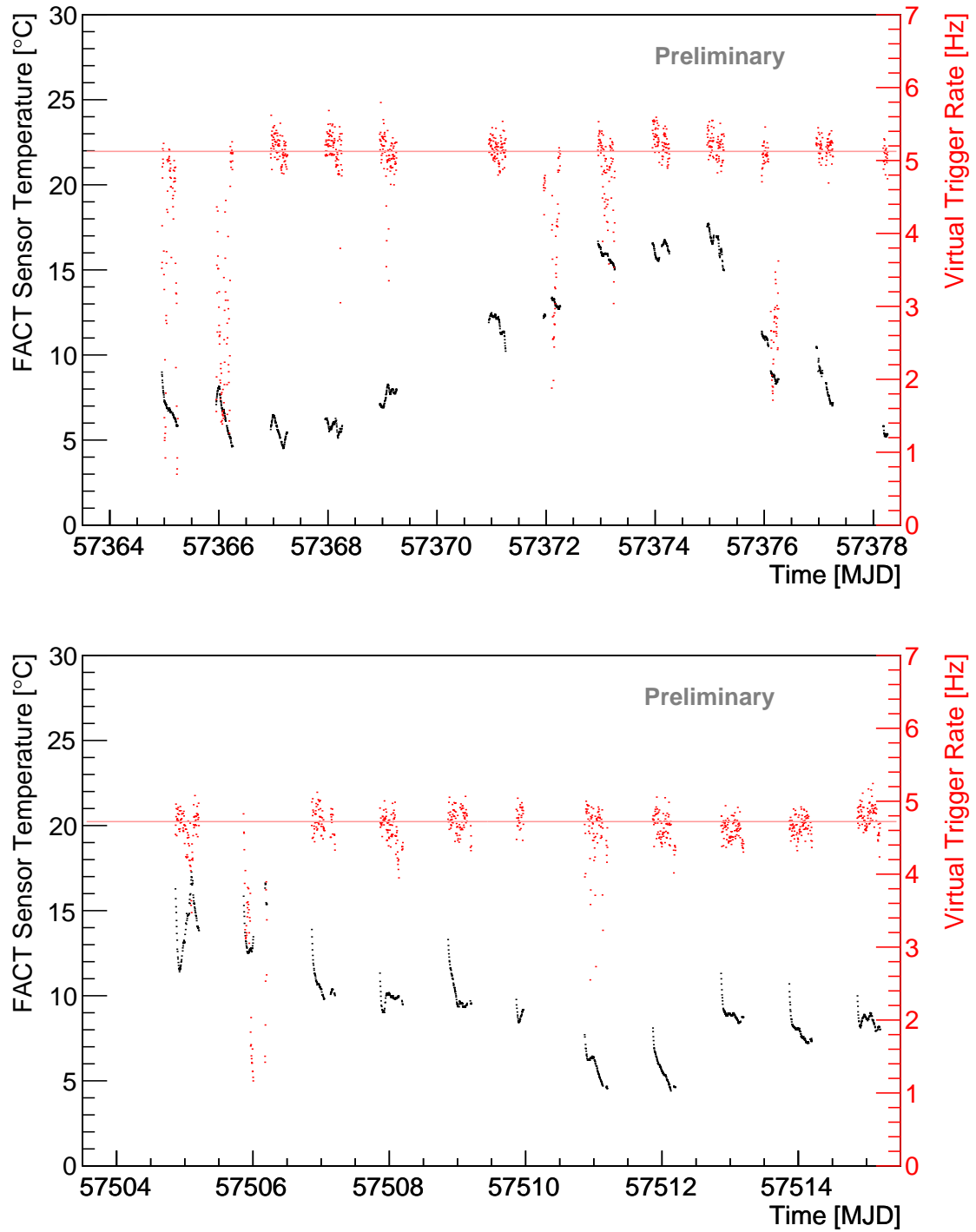


Figure 2: Virtual trigger rate (red) and sensor temperature (black) versus time for the datasets Dec.2015 (top) and Apr.2016 (bottom). The horizontal line corresponds to the average rate extracted from figure 4. No temperature dependence of the rate is visible.

3. Results

Figure 2 shows in red the virtual trigger rate and in black the average sensor temperature for each five minutes run taken with zenith distance smaller than 40° ⁵.

Several nights show many runs with significantly reduced virtual trigger rate (e.g. MJD 57506, 57364, 57366 and 57372), most probably due to increased atmospheric extinction of Cherenkov light as explained in [3]. The average virtual trigger rate changes between both periods due to the mentioned seasonal variation, but this is not important for this study. Figure 3 shows the virtual trigger rate versus the sensor temperature for both data periods. Despite a change of sensor temperature by more than 15°C within 10 days and up to 5°C within individual nights, there is no correlated change in the virtual trigger rate found.

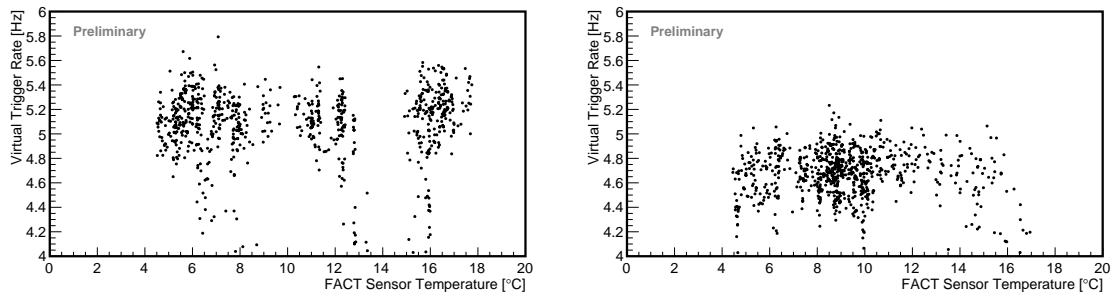


Figure 3: Virtual trigger rate versus sensor temperature for the datasets Dec2015 (left) and Apr.2016 (right). No correlation is seen (the highest temperatures of the right plot are dominated by bad atmospheric conditions).

This is a strong indication that despite large temperature variations, the Cherenkov yield (i.e. the number of Cherenkov photons measured from a given shower) does not significantly change.

Figure 4 shows the distribution of the virtual trigger rates for the two data periods. The tails to lower rates are most probably due to enhanced extinction of Cherenkov light due to clouds or calima⁶. Excluding these tails, a Gaussian was fitted to the distributions (red lines).

From the counted number of events within each run and assuming Poisson statistics for the arrival time of events, one can calculate the statistical uncertainty of the counting rate in each run. Subtracting in square this statistical uncertainty from the fitted width of the Gaussian, one can estimate the contribution not described by pure statistics:

$$\sigma_{fit} = \sqrt{\sigma_{stat}^2 + \sigma_{other}^2}$$

This is summarized in table 1.

From this one can estimate that there exists an $\approx 2\%$ contribution to the variation of the virtual trigger rate that cannot be explained by pure statistical fluctuations. There exist many short term effects that can contribute to this, among them (minor) variations of the atmospheric extinction and

⁵The only additional cut is to exclude runs where the veto against the MAGIC Lidar did not perform correctly and the data contain additional signals induced by this laser.

⁶A layer of Saharan dust sometimes occurring above the Canary Islands.

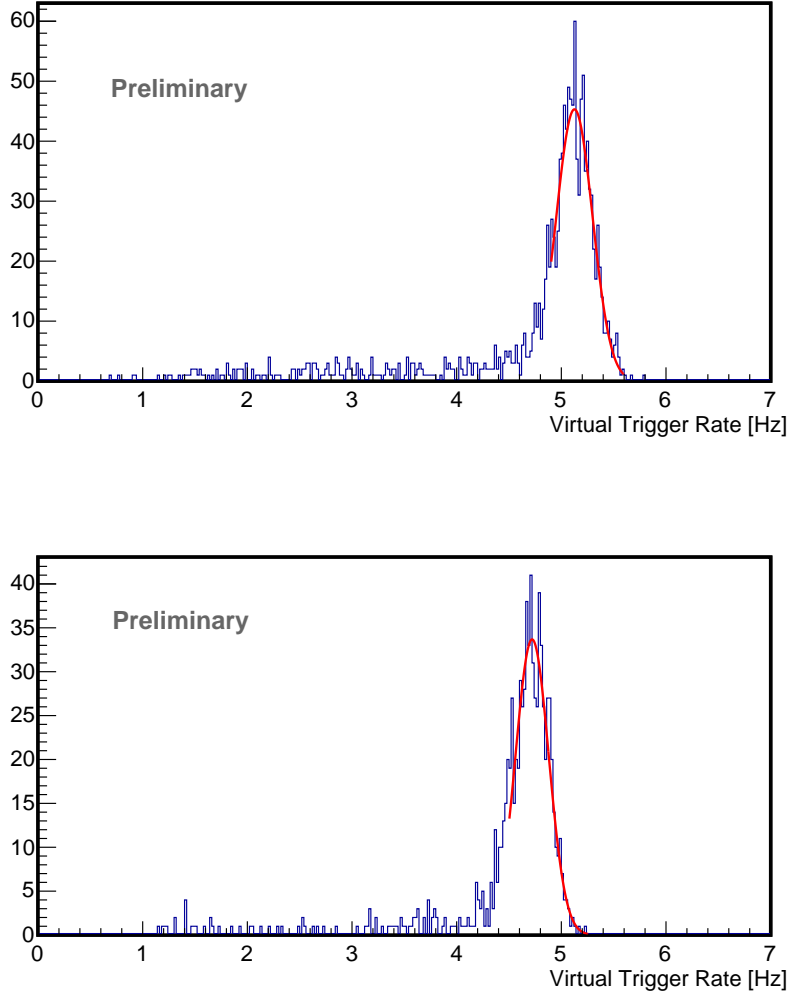


Figure 4: Fitting a Gaussian to the distributions of the virtual trigger rate for the datasets Dec.2015 (top) and Apr.2016 (bottom), excluding runs with significantly reduced rates. Fit parameters can be found in Table 1.

Period	Mean	σ_{fit}	$\sigma_{fit}\%$	$\sigma_{stat}\%$	$\sigma_{other}\%$
Dec.2015	5.13 ± 0.01	0.173 ± 0.007	3.36	2.64	2.08
Apr.2016	4.72 ± 0.01	0.159 ± 0.007	3.35	2.77	1.89

Table 1: Analysis of figure 4. The second and third columns contain the parameters of the Gaussian fit (red lines). The fourth column is this σ_{fit} given in percentage of the Mean. The fifth column is the statistical uncertainty for the Mean rate, assuming Poisson statistics and taking into account duration and deadtime of the runs. The last column gives an estimate of the remaining contribution from other reasons, by subtracting quadratic the values of column five from those of column four.

variations of the telescope sensitivity. In addition, the power supply of FACT can only be controlled with a finite resolution corresponding to a temperature change of $\approx 0.4^\circ\text{C}$, and the temperature is only sampled at 28 points on the sensor plane[2]. Therefore, the gain cannot be kept perfectly stable. This is probably a main contribution to the measured fluctuations.

Nevertheless, it has to be noted that such small fluctuations have negligible effect on any gamma-ray science performed with FACT.

4. Summary

We used the constant flux of charged cosmic ray particles as calibration device and investigated data taken when the temperatures of the SiPM sensors changed by more than 15°C within short time periods. FACT adjusts the voltage applied to the SiPM sensors to their temperature and DC current to keep the gain constant. We showed that remaining variations of the camera performance are negligibly small and are not dominated by higher order temperature dependent effects.

Acknowledgments

The important contributions from ETH Zurich grants ETH-10.08-2 and ETH-27.12-1 as well as the funding by the Swiss SNF and the German BMBF (Verbundforschung Astro- und Astroteilchenphysik) and HAP (Helmoltz Alliance for Astro- particle Physics) are gratefully acknowledged. Part of this work is supported by Deutsche Forschungsgemeinschaft (DFG) within the Collaborative Research Center SFB 876 "Providing Information by Resource-Constrained Analysis", project C3. We are thankful for the very valuable contributions from E. Lorenz, D. Renker and G. Viertel during the early phase of the project. We thank the Instituto de Astrofísica de Canarias for allowing us to operate the telescope at the Observatorio del Roque de los Muchachos in La Palma, the Max-Planck-Institut für Physik for providing us with the mount of the former HEGRA CT3 telescope, and the MAGIC collaboration for their support.

References

- [1] H. Anderhub et al. (FACT Collaboration), *Design and operation of FACT - the first G-APD Cherenkov telescope*, JINST 8 P06008 (2013)
- [2] A. Biland et al. (FACT Collaboration), *Calibration and performance of the photon sensor response of FACT — the first G-APD Cherenkov telescope*, JINST 9 P10012 (2014)
- [3] D. Hildebrand et al. (FACT Collaboration), *Using Charged Cosmic Ray Particles to Monitor the Data Quality of FACT*, these proceedings, ID 779